Journal of Low Temperature Physics
https://doi.org/10.1007/s10909-024-03180-4

Design Considerations for the Optimization of λ-SQUIDs

Constantin Schuster[1] · **Sebastian Kempf**[1,2]

Received: 25 October 2023 / Accepted: 15 June 2024

Abstract
Cryogenic microcalorimeters are key tools for high-resolution X-ray spectroscopy due to their excellent energy resolution and quantum efficiency close to 100%. Multiple types of microcalorimeters exist, some of which have already proven outstanding performance. Nevertheless, they cannot yet compete with cutting-edge grating or crystal spectrometers. For this reason, novel microcalorimeter concepts are continuously developed. One such concept is based on the strong temperature dependence of the magnetic penetration depth of a superconductor operated close to its transition temperature. This so-called λ-SQUID provides an in-situ tunable gain and promises to reach sub-eV energy resolution. Here, we present some design considerations with respect to the optimization of such a detector that are derived by analytic means. We particularly show that for this detector concept the heat capacity of the sensor should match the heat capacity of the absorber.

Keywords Superconducting microcalorimetre · λ-SQUID · SQUID · Cryogenic particle detector · Detector optimization

1 Introduction

Cryogenic microcalorimeters such as superconducting transition-edge sensors (TESs) [1, 2] or metallic magnetic calorimeters (MMCs) [3, 4] have proven to be outstanding tools for measuring the energy of X-ray photons with unprecedented precision. They rely on sensing the change in temperature of an X-ray absorber upon photon absorption using an extremely sensitive thermometer that is based either on a superconducting (TES) or paramagnetic (MMC) sensor material. Due to their unique combination of excellent energy resolution and quantum efficiency close to

✉ Constantin Schuster
constantin.schuster@kit.edu

[1] Institute of Micro- and Nanoelectronic Systems (IMS), Karlsruhe Institute of Technology (KIT), Hertzstrasse 16, 76187 Karlsruhe, Germany

[2] Institute for Data Processing and Electronics (IPE), Karlsruhe Institute of Technology (KIT), Hermann-von-Helmholtz-Platz 1, 76344 Karlsruhe, Germany

Published online: 01 July 2024

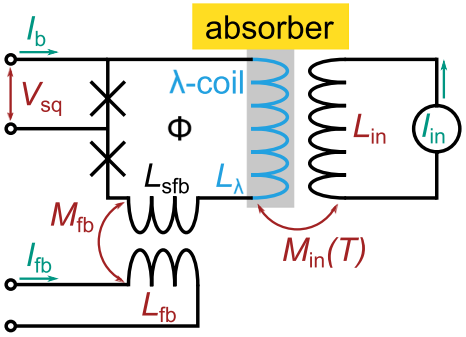

Fig. 1 Simplified equivalent circuit diagram of a λ-SQUID. Inductors shown in black are made from a superconductor with critical temperature T_c. The λ-coil displayed in blue is made from a different superconductor with critical temperature $T_{c,\lambda} \ll T_c$, and is in strong thermal contact with the absorber. The device is operated at temperature $T_0 \lessapprox T_{c,\lambda}$. A constant current I_{in} is injected into an input coil with inductance L_{in} and causes a temperature dependent magnetic flux within the SQUID loop via the temperature dependent mutual inductance $M_{in}(T)$

100%, they offer significant advantages as compared to state-of-the-art grating or crystal X-ray spectrometres [5]. Their quantum efficiency significantly relaxes the requirements on X-ray beam intensity, which especially benefits measurements on strongly diluted or radiation sensitive samples [6, 7]. Moreover, they cover the entire soft X-ray range [5] that is hardly accessible with both, grating and crystal spectrometers.

State-of-the-art TES- and MMC-based X-ray detectors achieve an energy resolution (FWHM) of 0.72 eV for 1.5 keV photons [8] and of 1.25 eV for 5.9 keV photons [9] at near-unity quantum efficiency. However, despite various ongoing developments, all targeting to improve the performance of these microcalorimeters, an energy resolution as low as 100 meV, required for investigating vibrations or *d*-*d*-excitations in soft X-ray spectroscopy or resonant inelastic X-ray scattering, has yet to be demonstrated. Against this background, we have recently proposed a novel type of microcalorimeter called λ-SQUID, that promises to provide the required energy resolution [10].

Figure 1 shows a simplified equivalent circuit diagram of a λ-SQUID. Similar to a conventional dc-SQUID, it consists of a superconducting loop interrupted by two Josephson tunnel junctions, each with critical current I_c, capacitance C_{JJ} and normal state resistance R. The superconducting loop is divided into two parts, i.e. a section L_{sfb} that couples to a flux biasing coil and a section with inductance L_λ, denoted as λ-coil, which couples to an external input coil. Most parts of the device, including both, the input coil and flux biasing coil, the section L_{sfb}, the Josephson junction electrodes, and the junction wiring, are made from a superconductor with a transition temperature T_c much larger than the device operating temperature T_0, i.e. $T_c \gg T_0$. In contrast, the λ-coil is made from a different superconductor with a transition temperature $T_{c,\lambda}$ that barely exceeds the operating temperature, i.e. $T_{c,\lambda} \gtrapprox T_0$. As a consequence, the magnetic penetration depth $\lambda(T)$ of the λ-coil and hence, the current distribution within the cross-section of the λ-coil shows a strong temperature

dependence that affects both, the inductance $L_\lambda(T)$ of the λ-coil as well as the mutual inductance $M_{\text{in}}(T)$ between the λ-coil and the input coil.[1] Assuming that a constant current I_{in} is injected into the input coil, the flux induced into the λ-SQUID then also becomes temperature sensitive: $\Phi(T) = I_{\text{in}} M_{\text{in}}(T)$. As in a typical dc-SQUID, this change in flux can be measured as a change in voltage across or current through the λ-SQUID, depending on the mode of operation. By bringing a suitable particle absorber with specific heat C_{abs} into close thermal contact with the λ-coil, the temperature rise upon particle absorption can be accurately detected and measured.

2 Design Considerations of the λ-coil

As the central sensing element, the λ-coil has an enormous influence on the performance of the λ-SQUID. Assuming a sophisticated readout chain in which the noise of subsequent amplifiers do not affect the noise performance of the λ-SQUID, e.g. by using an N-dc-SQUID series array as a first-stage low-temperature amplifier, the energy resolution ΔE_{FWHM} of a λ-SQUID is set by two noise contributions, i.e. thermodynamic energy fluctuations $S_{\text{E,TD}}$ caused by random energy fluctuations among the absorber, sensor and heat bath, and the noise contribution $S_{\text{E,SQ}}$ from the λ-SQUID itself. In the following, we will derive the conditions for the λ-coil which minimize the λ-SQUID noise contribution $S_{\text{E,SQ}}$.

We assume a hypothetical λ-SQUID as schematically shown in Fig. 2. For simplicity, the flux bias coil is neglected as it does not affect the temperature sensitivity. We consider a λ-coil entirely separable into small, identical unit elements, each with inductance $\tilde{L}$ and volume $\tilde{V}$. The loop comprises N parallel rows of M unit elements in series each, resulting in $N \times M$ unit elements in total. Each unit element couples to a segment of input coil with inductance $\tilde{L}_{\text{in}}$ via a mutual inductance $\tilde{M}_{\text{in}} = \kappa\sqrt{\tilde{L}\tilde{L}_{\text{in}}}$. Here, κ is the geometric coupling factor. We can thus conclude the following relations for the total loop inductance L and total volume V of the λ-coil and the combined mutual inductance M_{in} between the λ-SQUID and the input coil:

$$L = \frac{M}{N}\tilde{L} = \nu\tilde{L}, \tag{1}$$

$$V = MN\tilde{V} = \mu\tilde{V}, \tag{2}$$

[1] In our recent test device[10], niobium ($T_c \geq 8.9\,\text{K}$) is used for the majority of the device including the Josephson junction electrodes. The sensing element consists of aluminium ($T_{c,\lambda} \approx 1.2\,\text{K}$), resulting i n an operating temperature slightly above 1 K. For future iterations, sensor materials with a lower $T_{c,\lambda} \leq 100\,\text{mK}$ are desired to improve the detector performance[10], such as e.g. Au/Mo bilayer systems or elemental superconductors such as hafnium, iridium or tungsten. The sensor will be microfabricated using photolithography and sputter deposition or evaporation, while the absorber will be electroplated. Considered absorber materials are gold or bismuth with gold underlayer.

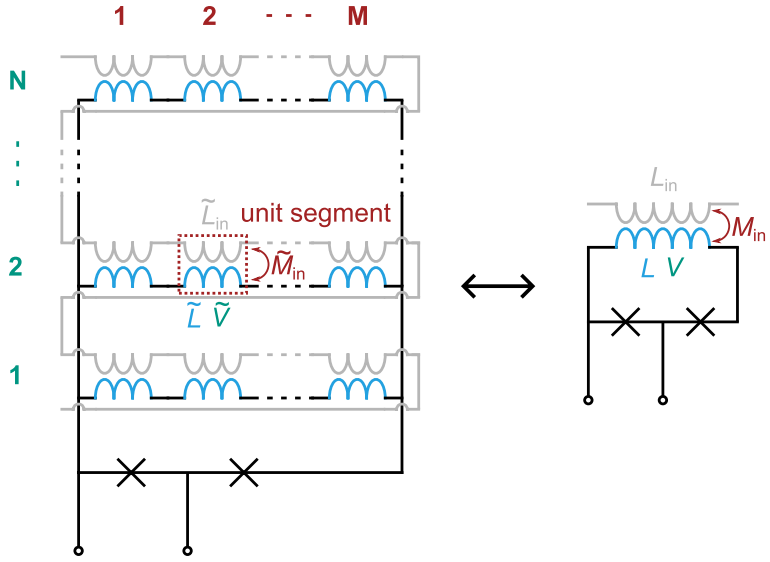

Fig. 2 Schematic circuit diagram of a hypothetical λ-SQUID. The SQUID loop consists of N identical segments connected in parallel, with each segment itself comprising M unit elements connected in series. One such unit element is framed in red. Each unit element has an inductance $\tilde{L}$ with volume $\tilde{V}$, and couples to a unit of input loop with inductance $\tilde{L}_{\mathrm{in}}$ with a mutual inductance $\tilde{M}_{\mathrm{in}}$. The total arrangement is equivalent to a single effective λ-coil with inductance L, volume V and mutual inductance M_{in} to an input coil with inductance L_{in}

$$M_{\mathrm{in}} = M\tilde{M}_{\mathrm{in}} = \sqrt{\nu\mu}\tilde{M}_{\mathrm{in}}. \tag{3}$$

Here, Eq. 3 can also be derived using $M_{\mathrm{in}} = \kappa\sqrt{LL_{\mathrm{in}}}$ with Eq. 1 and the fact that the total input inductance $L_{\mathrm{in}} = MN\tilde{L}_{\mathrm{in}} = \mu\tilde{L}_{\mathrm{in}}$ consists of a serial connection of the unit segment input coils $\tilde{L}_{\mathrm{in}}$. With only two free parametres to choose, we see immediately that we can not choose all three quantities independently. To quantify the remaining dependence, we have introduced the two parametres $\nu = M/N$ and $\mu = MN$ that fully define a specific layout of the λ-coil.

We use the geometric parameters ν and μ to express other relevant parameters: First, we assume that our λ-SQUID is optimized in terms of noise performance [11], i.e. the SQUID screening parameter is $\beta_{\mathrm{L}} = 2LI_{\mathrm{c}}/\Phi_0 = 1$ and the Stewart-McCumber parameter of the Josephson junctions is $\beta_{\mathrm{C}} = 2\pi I_{\mathrm{c}}R^2C_{\mathrm{JJ}}/\Phi_0 = 1$. Assuming an established fabrication process for Josephson junctions, the critical current is set by the junction area A_{JJ} and the critical current density j_{c} via $I_{\mathrm{c}} = A_{\mathrm{JJ}}j_{\mathrm{c}}$. The junction capacitance consequently is $C_{\mathrm{JJ}} = A_{\mathrm{JJ}}c^{\star}_{\mathrm{JJ}} = I_{\mathrm{c}}c^{\star}_{\mathrm{JJ}}/j_{\mathrm{c}}$, with the process-specific junction capacitance per unit area $c^{\star}_{\mathrm{JJ}}$. From the conditions $\beta_{\mathrm{L}}, \beta_{\mathrm{C}} = 1$ we conclude:

$$I_{\mathrm{c}} = \left[\frac{\Phi_0}{2\tilde{L}}\right]\frac{1}{\nu}, \tag{4}$$

$$R = \left[\sqrt{\frac{2j_c}{\pi\Phi_0 c_{JJ}^{\star}}}\tilde{L}\right]\nu. \tag{5}$$

In each expression, the term in brackets is independent of the specific design of the λ-SQUID, and depends only on fabrication parameters and the design of a unit element of the λ-coil.

The noise contribution $S_{E,SQ}$ caused by the λ-SQUID, expressed in fluctuations of the energy content, is given by the expression

$$S_{E,SQ} = S_{\Phi}\left(\frac{\partial\Phi}{\partial T}\frac{\partial T}{\partial E}\right)^{-2}. \tag{6}$$

Here, S_{Φ} denotes the magnetic flux noise of the SQUID. Moreover, $\frac{\partial\Phi}{\partial T}$ and $\frac{\partial T}{\partial E} = 1/C_{tot}$ are the temperature-to-flux transfer coefficient of the λ-SQUID and the inverse total heat capacity of the detector, respectively. For an optimized dc-SQUID, the flux noise can be approximated by $S_{\Phi} \approx 18k_B TL^2/R$ at the operating temperature T [12]. The total heat capacity of the detector comprises both, the absorber and the λ-coil, i.e. $C_{tot} = C_{abs} + \mu\tilde{V}c$, with c the specific heat per unit volume of the λ-coil. The temperature-to-flux transfer coefficient $\frac{\partial\Phi}{\partial T}$ of the λ-SQUID is given by

$$\frac{\partial\Phi}{\partial T} = I_{in}\frac{\partial M_{in}}{\partial T} = \left[I_{in}\frac{\partial\tilde{M}_{in}}{\partial T}\right]\sqrt{\mu\nu}, \tag{7}$$

where again, the term in brackets does not depend on the design of the λ-coil as a whole, but rather on the unit element. Using Eqs. 4 and 5 we obtain for the noise contribution

$$S_{E,SQ} = 18k_B T\sqrt{\frac{\pi\Phi_0 c_{JJ}^{\star}}{2j_c}}\tilde{L}\nu\left(\left[I_{in}\frac{\partial\tilde{M}_{in}}{\partial T}\right]\sqrt{\mu\nu}\frac{1}{C_{abs}+\mu\tilde{V}c}\right)^{-2} \tag{8}$$

$$= \left[18k_B T\sqrt{\frac{\pi\Phi_0 c_{JJ}^{\star}}{2j_c}}\frac{\tilde{L}}{I_{in}^2\left(\frac{\partial\tilde{M}_{in}}{\partial T}\right)^2}\right]\frac{\left(C_{abs}+\mu\tilde{V}c\right)^2}{\mu} = \eta g(\mu). \tag{9}$$

Here, we have introduced the substitutions

$$\eta = \left[18k_B T\sqrt{\frac{\pi\Phi_0 c_{JJ}^{\star}}{2j_c}}\frac{\tilde{L}}{I_{in}^2\left(\frac{\partial\tilde{M}_{in}}{\partial T}\right)^2}\right] \quad \text{and} \tag{10}$$

$$g(\mu) = \frac{\left(C_{abs}+\mu\tilde{V}c\right)^2}{\mu}. \tag{11}$$

We see that $S_{\mathrm{E,SQ}}$ neatly separates into a term η which depends only on the unit element, but is independent of the specific layout of the λ-coil, and a function $g(\mu)$, which contains the dependence of the λ-SQUID noise $S_{\mathrm{E,SQ}}$ on the arrangement of unit elements that comprises the λ-coil. It is interesting to note that only μ appears here, and that the parameter ν has dropped out. This can be understood as follows: An increase in ν causes a proportional increase in total inductance L and a rise of $M_{\mathrm{in}} \propto \sqrt{\nu}$. While the latter results in an increase of detector signal, the former affects the flux noise negatively. Ultimately, the signal-to-noise of the λ-SQUID remains unaltered by a change of the inductance L by varying the parameter ν as introduced above.

To minimize the noise level $S_{\mathrm{E,SQ}}$, we only have to consider the design parameter μ. Since, the prefactor η has no influence on this optimization, we restrict our efforts to the function $g(\mu)$ and find

$$\frac{\partial g(\mu)}{\partial \mu} = \frac{2\left(C_{\mathrm{abs}} + \mu\tilde{V}c\right)c\tilde{V}}{\mu} - \frac{\left(C_{\mathrm{abs}} + \mu\tilde{V}c\right)^2}{\mu^2} \tag{12}$$

$$\frac{\partial^2 g(\mu)}{\partial \mu^2} = \frac{2\left(c\tilde{V}\right)^2}{\mu} - \frac{4\left(C_{\mathrm{abs}} + \mu\tilde{V}c\right)c\tilde{V}}{\mu^2} + \frac{2\left(C_{\mathrm{abs}} + \mu\tilde{V}c\right)^2}{\mu^3} \tag{13}$$

for its first and second derivative. In this way, we find that the function $g(\mu)$, and thus the λ-SQUID energy noise contribution $S_{\mathrm{E,SQ}}$, has a minimum if the condition $\mu = \mu_{\mathrm{opt}}$ is satisfied, with

$$\mu_{\mathrm{opt}} c\tilde{V} = C_{\mathrm{sens}} = C_{\mathrm{abs}}. \tag{14}$$

Thus, we can conclude that the layout of the λ-coil should be chosen such that the total specific heat of the λ-coil exactly equals the specific heat of the absorber $C_{\mathrm{sens}} = C_{\mathrm{abs}}$. This resembles a well-known result for cryogenic microcalorimetres [13].

3 Conclusion

The recently proposed λ-SQUID is a superconducting microcalorimeter with in-situ tunable gain and, with a proper choice of absorber and sensor material, promises to reach sub-eV energy resolution. In preparation for such a demonstration, we have shown theoretical design considerations related to the optimization of the layout of the λ-coil, which is the fundamental sensing element of a λ-SQUID. By sub-dividing the λ-coil into a large number of small unit elements, we could abstract the layout of any possible design of the λ-coil for a given fabrication method, and describe the remaining degrees of freedom in the design process by two parametres μ and ν. When considering the influence of these parameters on the energy noise contribution $S_{\mathrm{E,SQ}}$ of the λ-SQUID, we draw two conclusions. First, the total inductance L of the λ-coil has no effect on the resulting energy

noise, and can thus be chosen freely. Second, the noise contribution $S_{\mathrm{E,SQ}}$ is minimized if the total volume of the λ-coil is chosen such that its specific heat directly equals that of the X-ray absorber: $C_{\mathrm{sens}} = C_{\mathrm{abs}}$.

Acknowledgements C. Schuster acknowledges financial support by the Karlsruhe School of Elementary Particle and Astroparticle Physics: Science and Technology (KSETA).

Author Contributions C.S. performed the mathematical derivations and prepared the figures. All authors contributed to the original idea and the main manuscript, both in writing and review.

Funding Open Access funding enabled and organized by Projekt DEAL.

Declarations

Conflict of interest The authors declare no conflict of interest.

References

1. K.D. Irwin, G.C. Hilton, in *Transition-Edge Sensors*. ed. by C. Enss (Springer, Berlin, 2005), pp.63–150. https://doi.org/10.1007/10933596_3
2. J.N. Ullom, D.A. Bennett, Review of superconducting transition-edge sensors for x-ray and gamma-ray spectroscopy. Supercond. Sci. Technol. **28**(8), 084003 (2015). https://doi.org/10.1088/0953-2048/28/8/084003
3. A. Fleischmann, C. Enss, G.M. Seidel, in *Metallic Magnetic Calorimeters*. ed. by C. Enss (Springer, Berlin, 2005), pp.151–216. https://doi.org/10.1007/10933596_4
4. S. Kempf, A. Fleischmann, L. Gastaldo, C. Enss, Physics and applications of metallic magnetic calorimeters. J. Low Temp. Phys. (2018). https://doi.org/10.1007/s10909-018-1891-6
5. J. Uhlig, W.B. Doriese, J.W. Fowler, D.S. Swetz, C. Jaye, D.A. Fischer, C.D. Reintsema, D.A. Bennett, L.R. Vale, U. Mandal, G.C. O'Neil, L. Miaja-Avila, Y.I. Joe, A. El Nahhas, W. Fullagar, F. Parnefjord Gustafsson, V. Sundström, D. Kurunthu, G.C. Hilton, D.R. Schmidt, J.N. Ullom, High-resolution X-ray emission spectroscopy with transition-edge sensors: present performance and future potential. J. Synchrotron Radiat. **22**(3), 766–775 (2015). https://doi.org/10.1107/S1600577515004312
6. S. Friedrich, Cryogenic X-ray detectors for synchrotron science. J. Synchrotron Radiat. **13**(Pt 2), 159–71 (2006). https://doi.org/10.1107/S090904950504197X
7. W.B. Doriese, K.M. Morgan, D.A. Bennett, E.V. Denison, C.P. Fitzgerald, J.W. Fowler, J.D. Gard, J.P. Hays-Wehle, G.C. Hilton, K.D. Irwin, Y.I. Joe, J.A.B. Mates, G.C. O'Neil, C.D. Reintsema, N.O. Robbins, D.R. Schmidt, D.S. Swetz, H. Tatsuno, L.R. Vale, J.N. Ullom, Developments in time-division multiplexing of X-ray transition-edge sensors. J. Low Temp. Phys. **184**, 389–395 (2016). https://doi.org/10.1007/s10909-015-1373-z
8. S.J. Lee, S.J. Adams, S.R. Bandler, J.A. Chervenak, M.E. Eckart, F.M. Finkbeiner, R.L. Kelley, C.A. Kilbourne, F.S. Porter, J.E. Sadleir, S.J. Smith, E.J. Wassell, Fine pitch transition-edge

sensor X-ray microcalorimeters with sub-eV energy resolution at 1.5 keV. Appl. Phys. Lett. **107**(22), 223503 (2015). https://doi.org/10.1063/1.4936793
9. M. Krantz, F. Toschi, B. Maier, G. Heine, C. Enss, S. Kempf, Magnetic microcalorimeter with paramagnetic temperature sensors and integrated dc-SQUID readout for high-resolution x-ray emission spectroscopy. Appl. Phys. Lett. **124**(3), 032601 (2024). https://doi.org/10.1063/5.0180903
10. C. Schuster, S. Kempf, SQUID-based superconducting microcalorimeter with in situ tunable gain. Appl. Phys. Lett. **123**(25), 252603 (2023). https://doi.org/10.1063/5.0179862
11. C.D. Tesche, J. Clarke, dc SQUID: noise and optimization. J. Low Temp. Phys. **29**, 301–331 (1977). https://doi.org/10.1007/BF00655097
12. B. Chesca, R. Kleiner, D. Koelle, in *The SQUID Handbook. Chap. SQUID Theory*. (Wiley, New York, 2004), pp.29–92. https://doi.org/10.1002/3527603646.ch2
13. D. McCammon, in *Thermal Equilibrium Calorimeters—An Introduction*. ed. by C. Enss (Springer, Berlin, 2005), pp.1–34. https://doi.org/10.1007/10933596_1